

Research of energy characteristics of power amplifier containing KNFS Nd:phosphate glass slabs and MIRO Silver foil reflectors at the “Luch” facility

I A Belov, S A Bel’kov, I N Voronich, S G Garanin, V N Derkach,
S V Koshechkin¹, M I Lysov, S S Markov and S V Savkin

Russian Federal Nuclear Center “All-Russian Research Institute of Experimental Physics”, pr. Mira 37, 607190 Sarov, Nizhnii Novgorod region, Russian Federation

oefimova@otd13.vniief.ru

Abstract. The amplifier elements upgrade at the “Luch” laser facility was carried out. Measurements showed that the upgrade of the amplifier elements resulted in the amplifier’s small signal gain coefficient K_0 increase from 12.9% to 14.3% depending on the capacitor charging voltage; the linear gain coefficient increase was about $g_0 \approx (6-8)\%$. Full-scale laser experiments at the facility showed the power amplifier gain coefficient increase consistent with active medium gain coefficient measurement results.

1. Introduction

Upgrade operations of amplifiers at the “Luch” facility [1, 2] were started in 2013. Elements upgrade operations included the replacement of amplifiers’ blastshields made of FLOAT glass by K-8 glasses with antireflection coatings, and the replacement of flat MIRO [3] foil reflectors by MIRO Silver [4] foil reflectors. Measurements of the gain coefficient showed that amplifier elements upgrade resulted in stored energy increase from 6.4% to 7.0%. The regular gain coefficient level of power amplifier under reduced flashlamp explosion fraction $f_x = 0.2$ (the capacitor charging voltage was equal to $U = 20$ kV) instead of 0.25 ($U = 22$ kV) was achieved in the full-scale experiments at the facility due to stored energy increase.

In the course of above mentioned work, the reequipment of the amplifiers with KNFS (KNFS-1 and KNFS-3) laser glass slabs [5] was carried out in 2015 at the “Luch” facility in the process of planned refit of the amplifiers. The reequipment with new slabs and other slabs rearrangement in the amplifiers were fulfilled in channel 1 (bottom channel) and channel 2 (top channel) of the facility. The main principles of slab placing into amplifiers were as follows. Firstly, all available laser slabs made of new KNFS-1 and KNFS-3 glass were placed into the channel 1. All other sites were equipped with KGSS-0180/35 glass slabs chosen among those that had been in use before. Secondly, among the slabs selected for channel 1 and channel 2, higher optical quality slabs were placed in the A1 amplifier, where the laser energy density was maximal. Overall, eight KNFS-1 slabs, eight KNFS-3 slabs and twenty KGSS-0180/35 slabs were placed in channel 1 and channel 2 of the amplifiers.

The active medium in the channel 1 of the A1 amplifier was formed with KNFS glass laser slabs, mainly KNFS-3 (seven KNFS-3 slabs and two KNFS-1 slabs) as a result of slabs rearrangement. The

¹ To whom any correspondence should be addressed.



active medium in the channel 1 of the A2 amplifier consisted of six KNFS-1 slabs, one KNFS-3 slab, and two KGSS-0180/35 slabs. In the channel 2 both A1 and A2 amplifiers were equipped with KGSS-0180/35 slabs.

Besides the reequipment of amplifiers with laser slabs made of KNFS laser glass, the total replacement of MIRO foil rhomb-shaped reflectors by MIRO Silver foil rhomb-shaped reflectors in flashlamp cassettes was carried out in the course of the amplifiers refit.

Experimental research of the active medium gain of the amplifiers was performed after the above described operations. The results are presented below.

2. The gain coefficient measurement experimental scheme

Gain coefficient measurements were performed by laser radiation amplification of a regular alignment laser in the amplifier channel. The amplifier channel contained 9 slabs. The scheme for the gain coefficient measurements was similar to the one described in [2, 3]. The principle scheme for the gain coefficient measurements is shown in Figure 1.

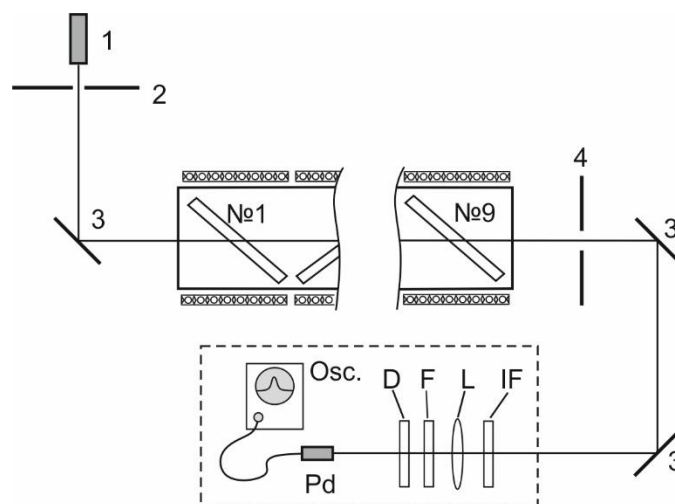


Figure 1. Principal optical scheme for the gain measurement. (1 – test laser, 2 – aperture diaphragm, 3 – dielectric mirrors, 4 – probing diaphragm, IF –interference filter, L – lens, F – optical filter, D – diffuser, Pd – photodiode FD256, Osc – oscilloscope TDS-3052).

The regular alignment laser (1) radiation with the wavelength of 1053 nm and beam size of $\approx 205 \times 205 \text{ mm}^2$ was passed through the amplifier. The probing diaphragm (4) (probing diaphragm diameter was equaled to 15 mm) was located in the optical path at the amplifier output to select the probe area on the amplifier aperture. The diaphragm (4) had also restricted pump light ingress into the registration scheme and acted as the selective diaphragm. After passing the diaphragm (4), laser beam with diameter 15 mm and power 1 mW (that corresponded to the oscilloscope signal value $U \approx 20 \text{ mV}$) was transported to the registration scheme by dielectric mirrors (3). The registration scheme was located in a separate room. The aperture diaphragm (2) with diameter 20 mm was placed in line with the diaphragm (4) at the amplifier input. The laser radiation was focused on the photodiode (Pd) by means of the lens (L) in the registration scheme. The interference filter (IF) ($\lambda = 1053 \text{ nm}$, $\Delta\lambda_{0.5} = 0.05 \mu\text{m}$) was placed before the lens to provide pump radiation interception. The IKS-7 optical filter (F) attenuated laser radiation power up to the desired level. The depolished glass diffuser (D) was placed before the photodiode. Registration scheme elements were protected from ambient illumination by means of a non-transparent tube. Measurements were performed with the time resolution $\sim 30 \text{ ns}$ using an FD256 silicone photodiode and a TDS-3052B oscilloscope.

Small signal gain coefficient measurements were carried out depending on the pump value at capacitor charging voltages 18, 20, 22, and 24 kV in channel 1 and channel 2 of the A1 amplifier at central aperture points and in the channel 1 of A2 amplifier at central aperture point. The geometric center of the fifth laser slab was taken as a central point of the amplifier optical aperture. Slabs pump was performed only in the A1 amplifier while performing the measurements on the A1 amplifier, and in the A2 amplifier while performing the measurements on the A2 amplifier.

The characteristic oscillogram of the amplified alignment radiation $U(t)$ and the oscilloscope zero readout taken 1 minute before the experiment without alignment irradiation and flashlamp pumping $U_0(t)$ are shown in Figure 2.

The amplified radiation pulse shape $U'(t)$ was calculated using the following formula:

$$U'(t) = U(t) - U_0(t). \quad (1)$$

To obtain the time dependence of the gain coefficient $K(t)$, the region before the moment of pump start was selected out of the distribution $U'(t)$, and the level of reference signal U_{ref} was evaluated under the average value in this region. The time dependence of the gain coefficient is presented in Figure 3. It was calculated according to the formula:

$$K(t) = \frac{U'(t)}{U_{\text{ref}}}. \quad (2)$$

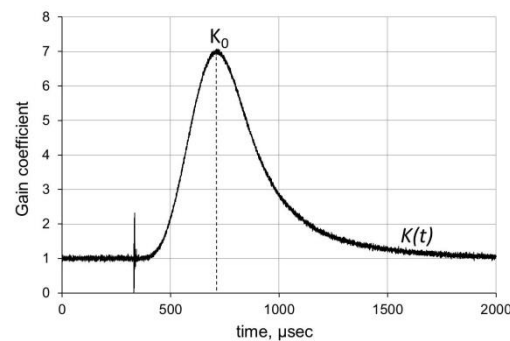
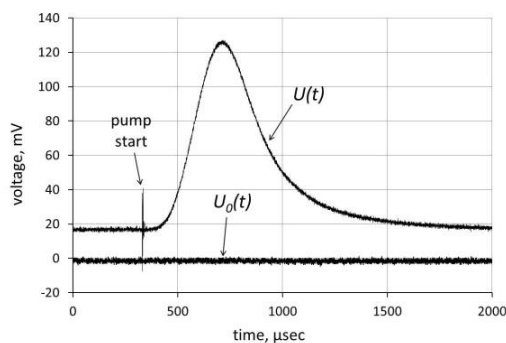


Figure 2. The characteristic oscillogram of temporal pulse shape of amplified radiation of the alignment laser $U(t)$, and the oscilloscope zero signal $U_0(t)$. **Figure 3.** Gain coefficient temporal dependence.

The small signal gain coefficient value K_0 corresponds to the distribution maximum of $K(t)$ and it was achieved in about 370 μs after the pump start (that approximately corresponds to monopulse arrival time in full-scale experiments). The measurement error of K_0 was about $\pm 5\%$. The small signal gain coefficient g_0 was calculated as:

$$g_0 = \frac{1}{L} \times \ln(K_0), \quad (3)$$

where $L = 43.2$ cm – active medium length (9 slabs at Brewster's angle). The relative measurement error of the linear gain coefficient g_0 was estimated by the formula:

$$\frac{\Delta g_0}{g_0} = \frac{\Delta K_0}{K_0 \times \ln(K_0)} \approx \pm 2.5\%. \quad (4)$$

3. Small signal gain experimental studies

Gain measurements in the channel 1 of the A1 amplifier (the A1 amplifier contained KNFS Nd-phosphate glass slabs) at capacitor charging voltages $U = 18, 20, 22,$ and 24 kV were carried out.

Obtained time dependences of the gain coefficient at capacitor charging voltages $U = 18, 20, 22,$ and 24 kV are presented in Figure 4. Figure 5 illustrates characteristic of the pump current pulse, the light pump pulse oscillogram registered in red spectral region in one of the experiments (behind the KS-13 filter), and the time dependence of the gain coefficient.

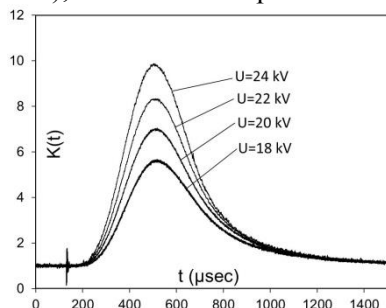


Figure 4. The time dependences of the gain coefficient at various capacitor charging voltages.

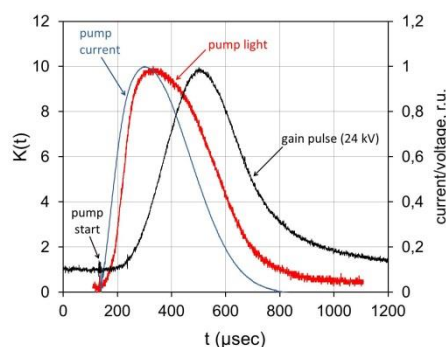


Figure 5. The time dependence of the gain coefficient; the light pump pulse oscillogram ($\lambda \geq 600$ nm) and the pump current oscillogram.

Gain coefficient measurement data at the central aperture point in the amplifier channel containing KNFS slabs are presented in Table 1. Defined capacitor charging voltages, values of electric energy delivered to a flashlamp E_{del} , values of small signal gain coefficients K_0 , and values of linear gain coefficient g_0 calculated according to small signal gain coefficients K_0 are presented in Table 1. The electric energy delivered to the flashlamp was calculated using formula:

$$E_{del} = \frac{T}{N} \cdot \sum_{i=1}^n \left[\frac{\left(\sum_{j=1}^m C_{ji} \right) \cdot U_i^2}{2} \right], \quad (5)$$

where $N=144$ – the number of flashlamps in 9 amplifier modules, $n=9$ – the number of amplifier modules, $m=4$ – the number of capacitors supplying pumping lamps of one of the amplifier module, C – value of capacitance supplying 4 flashlamp series chain (certified value), U – capacitor charging voltage at the moment of flashlamps firing, $T \approx 0.8$ [2] – the bank-to-lamp energy transfer efficiency.

Table 1. Gain data obtained in the amplifier channel containing KNFS glass slabs.

$U, \text{ kV}$	$E_{del}, \text{ kJ}$	K_0	$g_0 \times 10^2, \text{ cm}^{-1}$
18	5.4	5.7 ± 0.3	4.0 ± 0.1
20	6.6	7.1 ± 0.4	4.5 ± 0.1
22	8.0	8.3 ± 0.4	4.9 ± 0.1
24	9.5	9.7 ± 0.5	5.3 ± 0.1

Figure 6 shows the comparison of gain coefficient g_0 dependences on the delivered energy E_{del} , obtained after blastshields and flat reflectors replacement in 2013, and after equipping the amplifier with KNFS slabs and upgrade of the rhomb-shaped reflectors.

As shown in Figure 6, significant increase of linear gain coefficient was achieved as a result of the reequipping of the channel 1 with slabs made of KNFS laser glass and the replacement of rhomb-shaped reflectors in flashlamp cassettes. The increment of the linear gain coefficient g_0 value varied from $\approx 6.2\%$ to $\approx 8.4\%$ depending on the electric energy delivered to the flashlamps, while the electric energy E_{del} varied from ≈ 5.4 kJ to ≈ 9.6 kJ (charging voltage equalled to 18-24 kV).

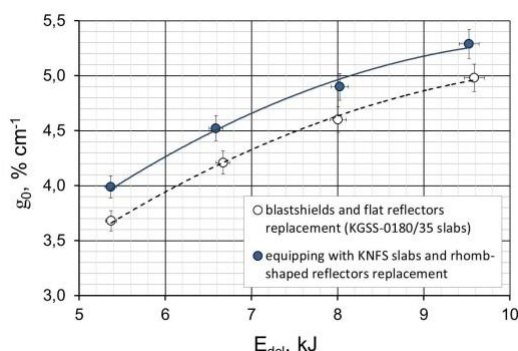


Figure 6. The gain coefficient dependence on the delivered energy before and after the amplifier's equipment with the KNFS slabs.

Significant increment of the gain coefficient value is unclear because technical requirements of the KGSS-0180/35 and KNFS laser slabs material are identical. The increase of the pump radiation flux after replacement of the MIRO foil rhomb-shaped reflectors by MIRO Silver foil rhomb-shaped reflectors was expected to be less than 3% (reflection coefficients of foils were equal to 95% and 98% respectively [4]).

Therefore, it was decided to carry out the study of the gain coefficient more thoroughly in order to allow to directly compare the values of the gain coefficients obtained on KNFS and KGSS-0180/35 glass laser slabs, eliminating the influence of the rhomb-shaped reflectors material.

3.1. Active medium gain coefficient research of different laser glass types

To exclude the impact of reflectors material, the gain coefficient measurements were carried out in A1 amplifier channel 2 containing KGSS-0180/35 slabs only. Since the gain studies of A1 amplifier channel 1 described above had been finished, a series of over 20 full-scale experiments run on the facility. Therefore, to correctly compare the KGSS-0180/35 and KNFS gain characteristics, after the measurements in A1 amplifier channel 2, the gain measurements were made in A1 amplifier channel 1 again.

It is obvious that both channels experience equal pump terms due to the amplifier symmetry.

Gain measurement results for channels 1 and 2 of A1 amplifier are given in Tables 2 and 3, respectively.

Table 2. Gains measured in the amplifier channel containing KGSS-0180/35 glass slabs.

U, kV	E_{del} , kJ	K_0	$g_0 \times 10^2$, cm^{-1}
18	5.4	5.0±0.3	3.7±0.1
20	6.6	6.0±0.3	4.2±0.1
22	8.0	7.3±0.4	4.6±0.1
24	9.5	8.4±0.4	4.9±0.1

Table 3. Gains measured in the amplifier channel containing KNFS glass slabs.

U, kV	E_{del} , kJ	K_0	$g_0 \times 10^2$, cm^{-1}
18	5.4	5.6±0.3	4.0±0.1
20	6.6	6.8±0.3	4.5±0.1
24	9.5	9.4±0.5	5.2±0.1

Figure 7 illustrates dependences of the gain coefficient on the energy delivered to the flashlamps for the KNFS glass amplifier channel and for the KGSS-0180/35 glass amplifier channel.

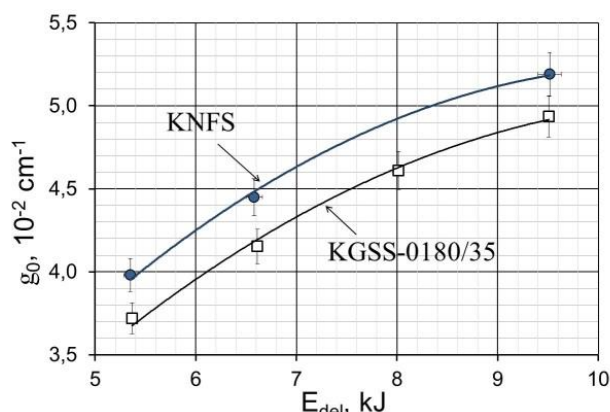


Figure 7. Dependences of the gain coefficient on the electric energy delivered to the flashlamps for the KNFS glass amplifier channel and for the KGSS-0180/35 glass amplifier channel.

As illustrated in Figure 7, values of linear gain coefficients obtained in the amplifier channel with KGSS-0180/35 glass active medium varied from $\approx 3.7 \cdot 10^{-2} \text{ cm}^{-1}$ to $\approx 4.9 \cdot 10^{-2} \text{ cm}^{-1}$ in the range of charging voltages from 18 to 24 kV (E_{del} from 5.4 to 9.6 kJ). Values of linear gain coefficients obtained in the amplifier channel with KNFS (mainly KNFS-3) glass active medium under the same pumping conditions varied from $\approx 4.0 \cdot 10^{-2} \text{ cm}^{-1}$ to $\approx 5.2 \cdot 10^{-2} \text{ cm}^{-1}$. Thus, linear gain coefficient values obtained for the KNFS glass active medium were by about 7% higher than that those for the KGSS-0180/35 glass slabs.

The gain coefficient value of the A2 amplifier channel 1 based on KNFS-1, KNFS-3, and KGSS-0180/35 slabs was also of interest.

Gain coefficient measurements in the A2 amplifier channel 1 with KNFS and KGSS-0180/35 slabs were carried out with the use of a similar scheme as for the A1 amplifier. Measurement data are presented in Table 4 and Figure 8.

Table 4. Gains measured in the amplifier channel containing KGSS-0180/35 and KNFS laser glass slabs.

U, kV	E_{del} , kJ	K_0	$g_0 \times 10^2$, cm $^{-1}$
18	5.4	5.3 ± 0.3	3.9 ± 0.1
20	6.6	6.5 ± 0.3	4.3 ± 0.1
22	8.0	7.8 ± 0.4	4.8 ± 0.1
24	9.5	9.0 ± 0.5	5.1 ± 0.1

Solid curve in Figure 8 shows g_0 gain coefficient dependence on the delivered energy for mixed type active media, dashed curves show $g_0(E_{del})$ dependences for KNFS only and for KGSS-0180/35 only containing amplifier channels. As shown in Figure 8, mixed media g_0 values are predictably situated in an intermediate position between special KNFS and KGSS gain results.

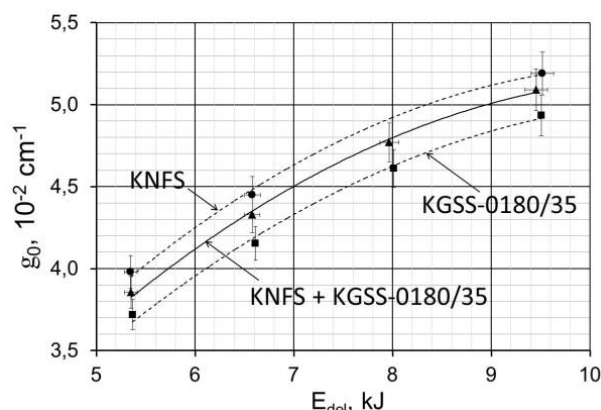


Figure 8. Gain coefficient dependence on the delivered energy for three amplifier channel configurations.

As shown in Figure 8, obtained values of linear gain coefficients predictably fall between the results for KNFS glass and KGSS-0180/35 glass.

3.2. Active media gain coefficient studies under different pumping conditions

Comparison of g_0 values in the A1 amplifier channel 2 obtained before rhomb-shaped reflectors upgrade in 2013 and after the reflectors replacement and laser slabs rearrangement in 2015 was provided to reveal the influence of the rhomb-shaped reflectors replacement on the value of the linear gain coefficient g_0 . The A1 amplifier channel 2 before and after the rearrangement of laser slabs (the reequipment of amplifiers by KNFS slabs) included only KGSS-0180/35 slabs.

Dependences of the gain coefficient on the delivered energy obtained before and after the replacement of rhomb-shaped reflectors in the A1 amplifier channel 2 are presented in Figure 9 (2013 and 2015). In the first case rhomb-shaped reflectors were made of MIRO foil, and in the second case, they were made of MIRO Silver foil.

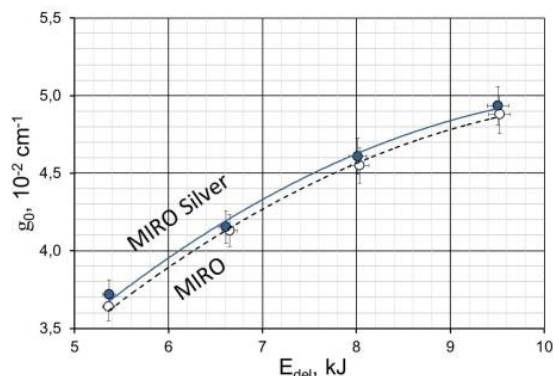


Figure 9. Dependences of the gain coefficient on the electric energy delivered to the flashlamps in the amplifier channel with MIRO and MIRO Silver foil rhomb-shaped reflectors.

As one can see from the graph presented in Figure 9, values of linear gain coefficient obtained after the replacement of the rhomb-shaped reflectors are situated higher than those obtained with formerly used reflectors. However, the difference of linear gain coefficient values is from about 1.1% to 1.6% over the whole pumping energy range. It is less than measurement error and processing error of experimental data.

4. The power amplifier efficiency increase at the “Luch” facility

Figure 10 shows dependences of the linear gain coefficient on the electric energy delivered to the flashlamps. These dependences were obtained before the amplifiers’ elements upgrade, after the

blastshields and flat reflectors replacement, and after the reequipping with KNFS slabs and the replacement of the rhomb-shaped reflectors.

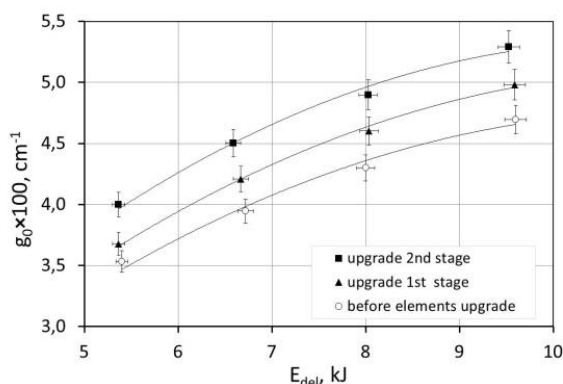


Figure 10. The dependence of the gain coefficient on the electric energy delivered to the flashlamps.

As can be seen from the graph presented in Figure 10, upgrade operations of amplifier elements performed at the first stage and at the second stage both allowed to significantly increase the value of the amplifier active medium gain coefficient at the “Luch” facility. The linear gain coefficient was increased from $\approx 12\%$ to $\approx 14\%$ after two upgrade stages over the delivered electric energy range from 5.3 kJ to 9.4 kJ. The value of the linear gain coefficient achieved about $5.3 \cdot 10^{-2} \text{ cm}^{-1}$ at the capacitor charging voltage 24 kV. Obtained gain coefficient increase (up to 14%) enabled receiving the regular output energy level while conducting the four-channel experiments at the facility, since it is known that operating under the four-channel regime results in the average linear gain coefficient decrease by about 15%.

There is no opportunity to measure the amplifiers active medium small signal gain coefficient value during each full-scale experiment carried out at the facility. Therefore, the power amplifier (implying both A1 and A2 amplifiers divided by cavity spatial filter) efficiency is most conveniently characterized by using the channel double-pass gain coefficient K_{12} for the purpose of control and analysis of the gain coefficient changing dynamics. The double-pass gain coefficient is determined from the formula:

$$K_{12} = \frac{E_{rev}}{E_{input}}, \quad (6)$$

where E_{rev} – the energy at the output of the second pass (or at the reverser input); E_{input} – the energy at the input of the laser channel.

Since the laser radiation amplification regime in the first 2 passes is linear, the double-pass gain coefficient K_{12} is related to small signal gain coefficients of A1 and A2 amplifiers according to the equation:

$$K_{12} = K_{A1}^2 \times K_{A2}^2 \times T \quad (7)$$

where $K_{A1} = \exp(g_{0A1} \cdot l)$ and $K_{A2} = \exp(g_{0A2} \cdot l)$ – small signal gain in A1 and A2 amplifiers, respectively, l – active medium length, T – laser channel double-pass transmission.

The dependence of the gain coefficient K_{12} on the experiment number in the full-scale experiments at the facility from 2011 till 2015 is presented in Figure 11. Periods before the upgrade of the amplifiers’ elements, after the first and second upgrade stages are also demonstrated in Figure 11.

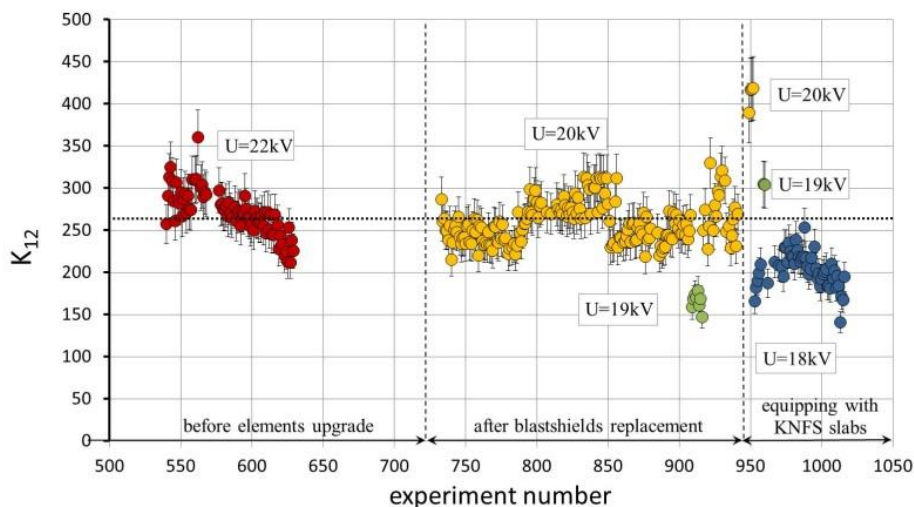


Figure 11. The dependence of the gain coefficient K_{12} on the experiment number.

As shown in Figure 11, the amplifier blastshields replacement made it possible to achieve regular level of the power amplifier gain coefficient ($K_{12} \approx 270$) in the full-scale experiments, i.e. regular output energy level at the same input signal, at a reduced value of the capacitor charging voltage $U=20$ kV, instead of 22 kV (under reduced flashlamps explosion fraction $f_x=0.2$, instead of 0.25). The realization of the second upgrade stage (i.e. the reequipping of amplifiers with KNFS slabs) resulted in the gain coefficient K_{12} increase up to ≈ 415 under $U=20$ kV. Obtained values of the gain coefficient K_{12} at the capacitor charging voltage 19 and 18 kV were $K_{12} \approx 305$ and 220, respectively. Thus, the second upgrade stage made it possible to achieve regular level of the laser channel output energy at the capacitor charging voltage $U=18$ kV ($f_x \approx 0.17$) with insignificant increase of the input signal from SRFS (supporting radiation forming system).

The facility power amplifier gain coefficient evolution after performing of two amplifiers upgrade stages is illustrated in Figure 12 as the dependence of the power amplifier gain coefficient K_{12} value on the squared capacitor charging voltage. Experimental and calculated results in Figure 12 are shown as filled and opened markers, respectively. Experimental dependences of the reverser input energy on the amplifier channel input energy in the full-scale experiments in the channel 1 at the facility are presented in Figure 13. The slopes of lines represented in Figure 13 correspond to the gain coefficient K_{12} .

Dependences in Figure 13 also indicate that the blastshields replacement allowed to reduce the charging voltage from 22 kV to 20 kV obtaining regular level of the power amplifier gain coefficient (dashed lines in Figure 13). This gain level occupies an intermediate position between $E_{rev}(E_{input})$ lines corresponding to data obtained after equipping amplifier with KNFS slabs at $U=18$ kV and 19 kV.

5. Conclusion

The amplifiers' elements upgrade was carried out. It included the equipment of the channel 1 with the KNFS laser glass slabs, the slabs rearrangement in the amplifiers, and the replacement of MIRO foil rhomb-shaped reflectors by MIRO Silver foil rhomb-shaped reflectors.

Active medium gain coefficient measurements in the channel 1 of the A1 amplifier were performed. The gain coefficient increase of 8.4% was obtained. The maximum value of the linear gain coefficient at the capacitor charging voltage 24 kV was about $g_0 \approx 5.3 \cdot 10^{-2} \text{ cm}^{-1}$.

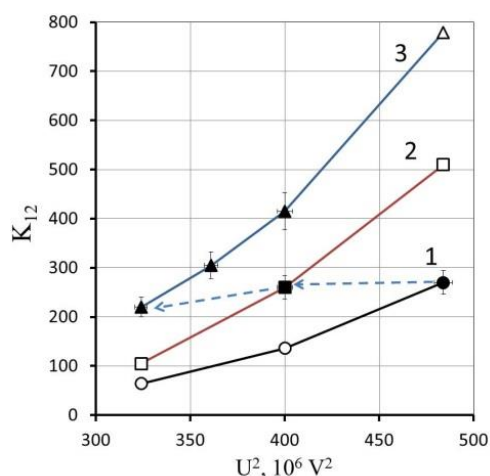


Figure 12. Dependence of K_{12} coefficient versus squared capacitor charging voltage (filled markers - experimental data; opened markers - calculated data). 1 – before the amplifiers elements upgrade, 2 – after the blastshields replacement, 3 – after the equipping of amplifiers with KNFS slabs.

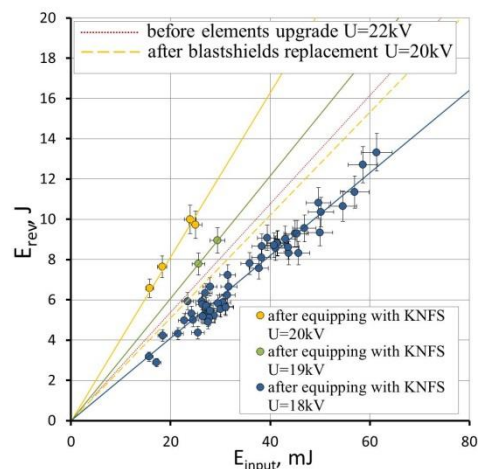


Figure 13. Experimental dependences of the energy at the reverser input on the energy at the channel input: red dashed line corresponds to the case before the amplifiers' upgrade, 22 kV; yellow dashed line corresponds to the case after the blastshields replacement, 20 kV; blue, green, and yellow solid lines correspond to the case after equipping with KNFS slabs, 18, 19, and 20 kV, respectively.

Gain coefficient studies in the amplifier channels based on KNFS and KGSS-0180/35 laser glass slabs were carried out. It was shown that the linear gain coefficient values of KNFS glass active medium were about 7% higher than the linear gain coefficient values for KGSS-0180/35 slabs. Gain coefficient measurements in the channel of the amplifier containing both KNFS glass laser slabs and KGSS-0180/35 laser glass slabs were carried out. Obtained linear gain coefficients values fall between the results for KNFS glass and KGSS-0180/35 glass.

Active media gain coefficient measurements data under different pumping conditions (different rhomb-shaped reflectors) were presented. It was shown that the rhomb-shaped reflectors replacement resulted in the about 1.5% increase of the gain coefficient.

It was demonstrated that the equipment of the amplifier modules with KNFS glass slabs, the replacement of the reflectors, and previous work with the blastshields replacement resulted in about 14% increase of the small signal linear gain g_0 .

References

- [1] Garanin S G, Zaretski A I, et al 2005 *Quantum Electron* **35** (4), 299-301.
- [2] Voronich I N, Galakhov I V, et al 2003 *Quantum Electron* **33** (6), 485-488.
- [3] Voronich I N, Garanin S G, et al 2004 *Quantum Electron* **34** (6), 509-510.
- [4] <http://www.alanod.com>
- [5] Avakyants L I, Ignatov A N, et al 2014 *Opt. Technol.* **81** (12) 719-722.